ACS APPLIED MATERIALS & INTERFACES

Research Article

www.acsami.org

Parasitic Currents Caused by Different Ionic and Electronic Conductivities in Fuel Cell Anodes

Maximilian Schalenbach,*[,†] Marcel Zillgitt,[†] Wiebke Maier,[†] and Detlef Stolten[†,‡]

[†]Forschungszentrum Jülich GmbH, IEK-3: Electrochemical Process Engineering, Wilhelm-Johnen Strasse, Jülich, NRW 52425, Germany

[‡]RWTH Aachen University, Chair for fuel cells, Templergraben 55, 52062 Aachen, Germany

Supporting Information

ABSTRACT: The electrodes in fuel cells simultaneously realize electric and ionic conductivity. In the case of acidic polymer electrolytes, the electrodes are typically made of composites of carbon-supported catalyst and Nafion polymer electrolyte binder. In this study, the interaction of the proton conduction, the electron conduction, and the electrochemical hydrogen conversion in such composite electrode materials was examined. Exposed to a hydrogen atmosphere, these composites displayed up to 10-fold smaller resistivities for the proton conduction than that of Nafion membranes. This effect was ascribed to the simultaneously occurring electrochemical hydrogen oxidation and evolution inside the composite samples, which are driven by different proton and electron resistivities. The parasitic electrochemical currents resulting were postulated to occur in the anode of fuel cells with polymer, solid oxide, or liquid alkaline electrolytes, when the ohmic drop of the ion conduction in the anode is higher with the anodic kinetic overvoltage (as illustrated in the graphical abstract). In this case, the parasitic electrochemical currents increase the anodic kinetic overpotential and the ohmic drop in the anode. Thinner fuel cell anodes with smaller ohmic drops for the ion conduction may reduce the parasitic electrochemical currents.

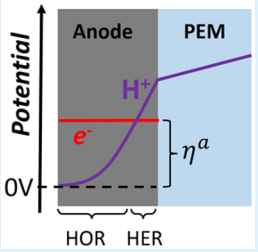

KEYWORDS: *polymer electrolyte membrane (PEM), hydrogen evolution reaction (HER), hydrogen oxidation reaction (HOR), catalyst layer, Nafion, proton resistance*

INTRODUCTION

In fuel cells, the electrodes must be simultaneously conductive to electrons and ions in order to promote the electrochemical reactions.[1−3] Furthermore, the reactants (hydrogen and oxygen) must gain access to the catalysts, which is ensured by the porosity of the electrodes.[4−6] In the case of acidic low-temperature polymer electrolyte membrane (PEM) fuel cells, precious platinum group metal catalysts are most commonly employed since they show the best activity and stability for the electrochemical conversion of hydrogen and oxygen to water.[7,8] To reduce the amount of such catalysts in the electrodes, nanometer catalyst particles are used to enhance the surface-to-weight ratio.[9,10] These nanoparticles are typically supported by carbon, which promotes electrical conductivity.[11] In fabricating electrodes for fuel cells, these carbon-supported catalysts are mixed with a polymer electrolyte binder, which conducts protons and supplies mechanical stability.[12,13] Electrodes, that are based on this combination of the catalyst, its support, and the polymer electrolyte binder are commonly referred to as catalyst layers.[12,13] Nafion (DuPont), a perfluorinated sulfonic acid, is typically used as the polymer electrolyte binder for the electrodes and the PEM.[14−16] With this structure of the catalyst layers, a triple phase boundary of a proton conducting phase, an electron conducting phase, and a porous phase for mass transport is provided at the catalyst particles.[2,4,5,17]

The aim of this study is to examine the interaction between the electrochemical hydrogen conversion, the ion conduction, and the electron conduction in fuel cell anodes, which is exemplified for the case of acidic polymer electrolyte catalyst layers. Hereto, the resistivities for the proton conduction of samples with equal compositions as catalyst layers for fuel cells were characterized in a hydrogen atmosphere. In addition, the resistivities of these samples for the electron conduction were measured since these will be shown to be decisive parameters for the examined interaction. In order to measure the contributions of both conductivities in a sample separately, we developed a novel technique that is illustrated in Figure 1. The influence of the ohmic drops for ion and electron conduction on the electrochemical hydrogen conversion in catalyst layers will be discussed to lead to parasitic electrochemical currents in fuel cell anodes, which increase the anodic overpotential.

EXPERIMENTAL SECTION

Hot-pressed composite samples consisting of Nafion binder and HiSpec9100 (Johnson Matthey) carbon-supported platinum fuel cell catalyst were examined in this study. The procedure of producing the samples is discussed in the Supporting Information. Figure 1 shows the setups used to characterize the proton and electron conduction of these samples. In order to determine the electrical resistivities of the samples, these were embedded into a plate capacitor geometry, and the direct current (DC) resistance was measured (Figure 1C). To avoid

Received: March 12, 2015
Accepted: July 8, 2015
Published: July 8, 2015

DOI: 10.1021/acsami.5b02182
ACS Appl. Mater. Interfaces 2015, 7, 15746−15751

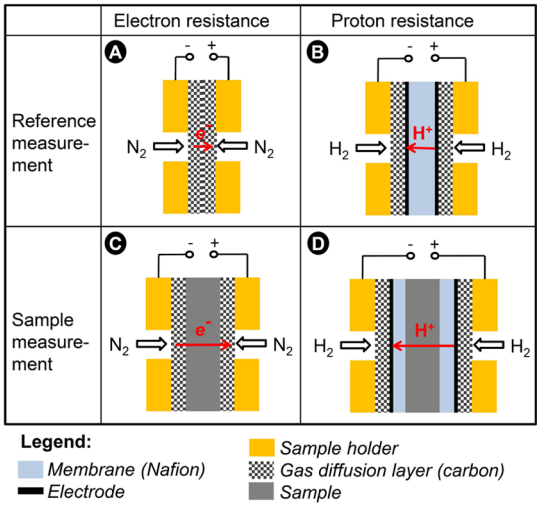

Figure 1. Schematic illustrations of the setups A–D used for the measurements. In setup B and D, the sample holders with the probes were immersed in a hydrogen atmosphere. Further information on the experimental setup is given in the Supporting Information.

electrochemical reactions of ambient gases in the samples, which would give rise to ionic conductivity, the measurements were conducted in an inert nitrogen atmosphere. When the samples were polarized in terms of their ionic charge, the measured current was attributable solely to their electrical conductivity. Reference measurements in the form of setup A (Figure 1A) were conducted, where the resistances of the apparatus, contacts, and cables were measured. The resistance of a sample R_s was then determined by

$$R_s = R_p - R_r \quad (1)$$

where R_p denotes the resistance of the probe measurement (with the sample) and R_r the resistance of the reference measurement (without the sample). The resistances of the cables of the apparatus included both R_p and R_r. By including the sample geometry, the resistivity ρ of a sample was determined by

$$\rho = R_s \frac{A}{d} \quad (2)$$

where d denotes its thickness and A its area. The conductivity equals the inverse resistivity.

To measure the proton conductivity of the composite samples, the same plate capacitor geometry as employed for the measurement of the electrical conductivity was used. However, the samples were hot-pressed between two Nafion NR212 proton exchange membranes (Figure 1D). In addition, these membranes were covered with fuel cell catalyst layers as electrodes. The electrically insulating membranes between the electrodes and the samples prohibited electron conduction through the probes, which are in the case of the proton conduction defined as the assembly of the electrodes, the membranes, and the samples. In a humidified hydrogen atmosphere a DC current applied to the electrodes led to proton permeation through the probes. Hydrogen was thus oxidized at the anode (+)

$$H_2 \rightarrow 2H^+ + 2e^- \quad (3)$$

while protons were reduced at the cathode (−) via the reversed reaction pathway. While the measurements were being taken, the conditions of an operating fuel cell were simulated in terms of temperature and relative humidity. In order to verify the absence of electric shorts between the electrodes, the DC resistances of the probes were measured in a nitrogen atmosphere to be infinite, as discussed in the Supporting Information. Gas diffusion layers of carbon on each side of the plate capacitor were used for electric contacting of the samples and uniform gas distribution. The ohmic drops at the probes were measured using direct currents (DCs), while the resistances of contacts, wires, and the carbon papers also contributed. These additional contributions were determined using reference measurements, where resistance of the same setup without the sample was measured (Figure 1B). The resistances of the samples were determined using eq 1. A detailed discussion of the equivalent circuit diagram for DC and alternating current (AC) measurements, the setup, the sample production, and the experimental realization can be found in the Supporting Information.

RESULTS AND DISCUSSION

In the following, measurements of electron and proton resistivities of composite samples which consist of Nafion binder and HiSpec9100 (Johnson Matthey) carbon-supported platinum fuel cell catalyst will be presented. These composite samples had a Nafion content of either 28, 33, or 38 wt %. As discussed in the Supporting Information, these values were positioned around the optimum Nafion content for PEM fuel cell catalyst layers that was reported in the literature. The measured resistivities of the samples to protons will be discussed and correlated with parasitic electrochemical currents that are caused by the electrochemical hydrogen oxidation and evolution inside the samples. Finally, the occurrence of these parasitic electrochemical currents in the anode of fuel cells will be postulated and discussed.

Resistivities of the Samples for the Electron and Proton Conduction. Table 1 shows the measured resistivities for the electron conduction through the samples. These measurements were performed using setup C, while the resistance determined by the reference measurements with setup A was subtracted (eq 1). Morris et al.[18] reported similar values and examined the influence of temperature and relative humidity on the electrical conductivity in detail. The Nafion binder in the samples is an electrical insulator. Electron conduction through the sample under direct current (DC) only takes place with the carbon particles and the catalyst in the samples. When the Nafion content of the samples is enlarged, the probability that the randomly distributed carbon particles with the catalyst are in contact with one another decreases. As a result, the measured electrical resistivity of the samples increased with higher Nafion contents.[18]

Table 1. Electrical Resistivities of Samples with Nafion Contents of Either 28, 33, or 38 wt % at Room Temperature Measured with Setup C, While Setup A Served as a Reference Measurement[a]

Nafion (wt %)	ρ (Ω cm)
28	0.33 ± 0.03
33	0.38 ± 0.02
38	0.59 ± 0.17

[a]The errors were determined by the standard deviation from five different samples measured.

Proton conduction in Nafion occurs in an aqueous phase formed by water channels.[19,20] The hydration level of Nafion increases with higher relative humidity of the ambient gases.[21−23] Figure 2 shows a decreasing measured proton resistivity of the Nafion NR212 (DuPont) membranes (approximately 55 μm in the fully hydrated state[24]) with higher relative humidity of the ambient hydrogen atmosphere and the resulting increased water uptake of the samples, which agrees with the values reported in the literature.[25,26] These measurements were conducted using setup B. To determine the proton resistivity of the Nafion membrane samples (eqs 1 and

DOI: 10.1021/acsami.5b02182
ACS Appl. Mater. Interfaces 2015, 7, 15746−15751

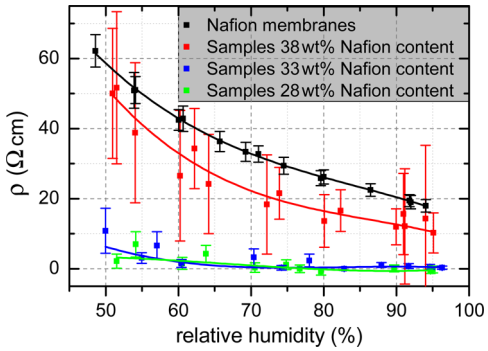

Figure 2. Measured resistivities of the proton conduction through Nafion membranes and of samples with either 28, 33, or 38 wt % Nafion content as a function of relative humidity at 80 °C.

2), reference measurements of the electrical resistances of the apparatus and the contacts were performed using setup A. The resistivity of the proton conduction of the probes with the samples in between the Nafion NR212 membranes was measured using setup D. Hereto, the resistance measured with setup B served as the reference (eq 1). The measurement error was determined by the standard deviation of five samples, while the influence of relative humidity on the measured proton resistivity of the samples was characterized by polynomial fits. The fit parameters and further information on the measurement procedure are given in the Supporting Information.

The samples with 38 wt % Nafion binder showed larger resistivities for proton conduction than those with 28 and 33 wt %. The latter samples with these lower Nafion contents had within the measurement precision equal resistivities that were approximately ten times smaller than those of the Nafion membranes. Boyer et al.[27] showed contrary results, where the resistivity for the proton conduction of the catalyst linearly increased with the Nafion content. In the setup of Boyer et al., the samples were also embedded in between two Nafion membranes, while hydrogen was supplied at the anode and oxygen at the cathode. The reaction was driven by the electrochemical potential of reactants (hydrogen and oxygen), while the resistances of the samples were determined by analyzing the voltage−current characteristic. Moreover, in his setup, the catalyst layer embedded between the Nafion membranes was sealed from the gases at the electrodes. Accordingly, the main difference between the setup of Boyer et al. and the setup presented in this study is that the samples measured in this study were in direct contact with a hydrogen atmosphere. Moreover, in this setup the electrochemical reactions at the electrodes were driven by an applied voltage, realizing an electrolysis cell in the form of an electrochemical hydrogen pump.[28] The different setups in the form of the fuel cell and the electrochemical hydrogen pump led to contrary potential distributions in the probes, which will be discussed in the following section. Moreover, in the following section the small resistivities of the samples measured in this study will be ascribed to the electrochemical conversion of hydrogen inside the samples.

Electrochemical Hydrogen Conversion Inside the Samples. The measured sample resistivities to electrons were at least 25 times smaller than the measured resistivities of the Nafion membranes to protons (Table 1, Figure 2). In the samples, the geometric restrictions of the proton conduction and the reduced volumetric Nafion content further increase the proton resistivities. On the basis of the results of Boyer et al.,[27] the proton resistivity of catalyst layers with the considered Nafion contents is at least 25 Ω cm, which means an at least 40 times larger ohmic drop of the proton conduction than that of the electron conduction through the samples (referring to electric resistivities stated in Table 1). The potential differences between the ionic phases and the electric phases of the samples resulting from the different resistivities are illustrated in Figure 3. These potential differences led to the electrochemical

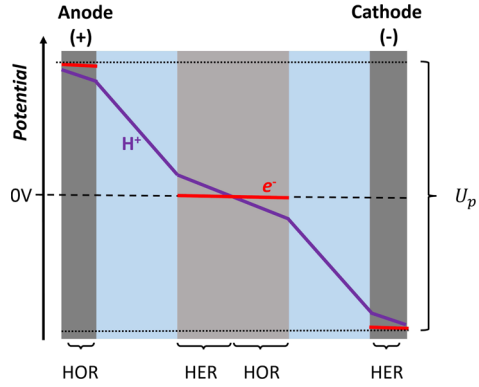

Figure 3. Schematic illustration of the qualitative potential distribution in the probes of setup D. The potential refers to the equilibrium potential of the hydrogen-proton redox couple (eq 3) in the middle of the sample, which is indicated by a dotted black line. The total potential difference at the probe equals the applied voltage U_p at the probes. Red: Potential of the electric phases. Purple: Potential of the ionic phases. Light blue area: Membranes. Light gray area between the light blue areas: Sample. Dark gray areas: Electrodes of the electrochemical hydrogen pump.

conversion of hydrogen within the samples, as discussed in the following. When the potential of the electric phase is higher than that of the ionic phase, the hydrogen oxidation reaction (HOR) can take place at the platinum catalyst[28] (eq 3). In the case of a lower potential of the electric phase than that of the ionic phase, the protons of the ionic phase can be reduced to hydrogen by the reversed reaction pathway.[28] This reaction is commonly referred to as hydrogen evolution reaction (HER).

At the side of the sample which faced the anode of the electrochemical hydrogen pump, the electric phase has a smaller potential than that of the ionic phase. Thus, at this side of the sample protons can be reduced to hydrogen. At the other side of the sample, the trend for the potentials is contrary, which means that hydrogen can be oxidized to protons. Driven by the potential differences of both phases, the HER and the HOR took place inside the samples. Consequently, a proton flux and an electron current from the region of the HOR to that of the HER permeated through the samples. This current inside the samples is defined as the parasitic electrochemical current I_x. In summary, at the side of the sample that faced the anode of the electrochemical hydrogen pump the HER took place, while at the anode itself the HOR occurred. This contrary trend of the reactions is also valid for the side of the sample that faced the cathode of the electrochemical hydrogen pump. Thus, the proton flux and electron current that resulted by the electrochemical hydrogen conversion inside the sample were in the opposite direction to that between the electrodes of the electrochemical hydrogen pump. Consequently, the current between the electrodes I equals the sum of the current that permeated in the form of protons through the sample I_{H^+} and the parasitic electrochemical current

DOI: 10.1021/acsami.5b02182
ACS Appl. Mater. Interfaces 2015, 7, 15746−15751

$$I = I_{H^+} + I_x \quad (4)$$

As a result, the current that permeated in the form of protons through the sample was smaller than the current which permeated between the electrodes of the electrochemical hydrogen pump.

Under current, the potential differences between the electric phase and the ionic phase in the samples increased with higher proton resistivities of the ionic phase, which consequently increased the driving force for the parasitic electrochemical currents. On the basis of the results of Boyer et al.,[27] the proton resistivity of the fuel cell catalyst layer increases with lower Nafion contents. Thus, assuming the same behavior for the samples measured, the ohmic drop for the proton conduction through the samples increased with lower Nafion contents. Accordingly, the driving force for the electrochemical currents inside the samples increased when their Nafion content was reduced. As a result, the samples with lower Nafion content had probably higher parasitic electrochemical currents which decreased the resistance measured (Figure 2). In addition, the parasitic electrochemical current might be diffusion limited by the concentration of hydrogen at the side of the sample where the HOR takes place. At the side of the sample where the HER took place hydrogen must permeate to the side where HOR occurred in order to enable the parasitic electrochemical current. A smaller Nafion loading of the samples might have increased the porosity and thus led to an increased permeability, which consequently increased the hydrogen permeation flux through the samples. As a result, the parasitic electrochemical currents might have increased with lower Nafion contents and the larger hydrogen permeabilities resulting.

Transfer of the Results to Fuel Cells. The measured lower resistivities of the samples in the hydrogen atmosphere than the resistivities of the Nafion membranes were thus far attributed to the electrochemical hydrogen oxidation and evolution inside the samples and the parasitic electrochemical current resulting. In order to transfer these results to the catalyst layers in fuel cells, the differences of the setup used in this study and that of fuel cells must be considered in detail. The setup D used for the measurements discussed above consisted of an electrochemical hydrogen pump, where a voltage was applied to the electrodes. As a result, the protons permeated from the anode to the cathode. In a fuel cell, the reaction is driven by the potential difference that comes from the hydrogen supplied at the anode and the oxygen supplied at the cathode. In both electrochemical devices the protons permeate from the anode to the cathode. However, in the case of the fuel cell, the anodic potential is lower compared to that of the cathode, while the relation of the potentials between both electrodes of the electrochemical hydrogen pump is contrary. Consequently, the ohmic drop of the proton conduction in fuel cells leads to a higher potential of the protons in the membrane compared to those at the anode, while in the case of the electrochemical hydrogen pump this relation is also contrary. Figure 3 and Figure 4 illustrate these trends.

The driving force for the electrochemical conversion inside the samples was thus far attributed to the potential difference between the electric phase and the ionic phase that originated from the different ohmic drops in both phases. These differences of the ohmic drops also occur in fuel cell catalyst layers. At the anode in a fuel cell, hydrogen is oxidized, which

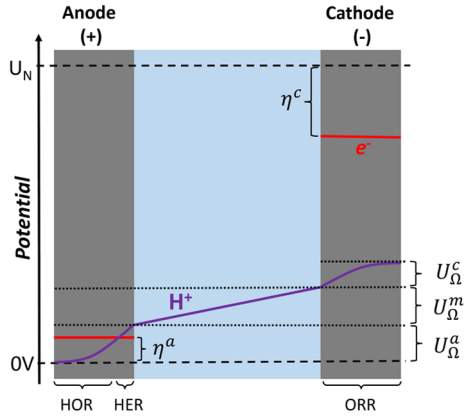

Figure 4. Schematic illustration of the qualitative distribution of the potential of the ionic phase and the electric phase in fuel cells. Hereto, the potential as a function of the distance refers to the potential of the protons at the side of the anode that faces the gas diffusion layer. An enlarged section of the anode region is shown in the graphical abstract. Red: Potential of the electric phase. Purple: Potential of the ionic phase. Light blue: PEM. Gray: Electrodes.

means that the mean potential of the electric phase must be higher than that of the ionic phase. However, due to the ohmic drop of the proton conduction, the potential of the ionic phase increases with smaller distances to the interface of the anode to the membrane (Figure 4). As a result, when the difference of the ohmic drops caused by the proton conduction and the electron conduction is higher than the kinetic overvoltage of the HOR, the ionic phase can have at least partially in the region close to the PEM a higher potential than that of the electric phase (Figure 4). In this region the HER thus can take place. Accordingly, a parasitic electrochemical current inside the anodic catalyst layer can cause exchanges of electrons and protons between the regions where the HOR and the HER take place. Referring to the potential distribution in the anodic catalyst layer where these reactions can occur, parasitic electrochemical currents within the anode are in the same direction as the proton flux caused by the electrochemical reaction between the electrodes. The proton flux through the catalyst layer increases with smaller distances to the PEM, as more of the reactants are electrochemically converted.[1] On the basis of Ohm's law, a nonlinear potential distribution of the ionic phase in the catalyst layers results,[1] as qualitatively illustrated in Figure 4.

Thus far, the occurrence of parasitic electrochemical currents as a result of the electrochemical hydrogen conversion inside the anodic catalyst layer of fuel cells was postulated. Normalized to the cell area of the fuel cell, the parasitic electrochemical current I_x can be expressed as the parasitic electrochemical current density j_x. In a fuel cell, the open-circuit voltage U_{OCV} is the maximum voltage which can be gained by a fuel cell.[29] The kinetic overvoltages and ohmic losses increase with the current density j between the electrodes and lead to a reduction of the cell voltage U_{cell} of the fuel cell[30,31]

$$U_{cell} = U_{OCV} - \eta^a(j + j_x) - U_\Omega^a(j + j_x) - U_\Omega^m(j) - \eta^c(j) - U_\Omega^c(j) - U_{mass} \quad (5)$$

where η^a denotes the anodic kinetic overvoltage, η^c the cathodic kinetic overvoltage, U_Ω^a the ohmic drop of the proton conduction in the anodic catalyst layer, U_Ω^c the ohmic drop of the proton conduction in the cathodic catalyst layer, U_Ω^m the

DOI: 10.1021/acsami.5b02182
ACS Appl. Mater. Interfaces 2015, 7, 15746−15751

ohmic drop of the proton conduction in the membrane, and U_{mass} the mass transport losses. In the latter equation, the ohmic drops for the electron conduction in the catalyst layers were neglected since these were discussed to be at least 40 times smaller than that of the proton conduction. As a result of the parasitic electrochemical current in the anode, the proton current that flows through the anode is larger than the current between the anode and the cathode. Accordingly, the ohmic drop of the proton conduction through the anode and the kinetic losses at the catalyst increase by the parasitic electrochemical currents. An increase of the anodic overpotentials results. To summarize, the following conclusion can be drawn:

- Parasitic electrochemical currents caused by the electrochemical hydrogen oxidation and evolution can occur in the anode of PEM fuel cells, when the kinetic overvoltage of the hydrogen oxidation is smaller than the difference of the ohmic drops of the proton conduction and the electron conduction inside the anodic catalyst layers. As a consequence, hydrogen can be evolved at the side of the anodic catalyst layer that faces the PEM.
- When parasitic electrochemical currents occur in the anodic catalyst layer, these lead to an increase of the proton flux and the electron current. As a result, the ohmic drops for the proton and the electron conduction in the anodic catalyst layer increase.
- The higher reaction rates caused by parasitic electrochemical currents increase the kinetic losses for the electrochemical hydrogen conversion in the anodic catalyst layer.
- As a result of the enlarged ohmic and kinetic losses, the parasitic electrochemical currents increase the anodic potential and thus reduce the efficiency.
- The ohmic drop for the proton conduction in the anode increases with thicker catalyst layers, which consequently lead to larger parasitic electrochemical currents.
- Catalyst particles which are connected to the electrolyte but not to the electric phase can be involved in the electrochemical hydrogen conversion (as shown by the samples between the membranes), which are a result of potential differences in the ionic phase at different parts of the surface of the catalyst particle. These electrochemical reactions do not contribute to the electrochemical reactions between the electrodes in fuel cells. However, these catalyst particles can contribute to the mass transport.

In solid oxide fuel cells,[32−34] operation temperatures of 600−1000 °C[35] realize small kinetic overpotentials for the electrochemical hydrogen conversion even without platinum metal group based catalyst,[36,37] while the ionic resistance of the solid oxide electrolyte for the oxygen ion conduction is rather high.[38,39] In the case of low-temperature alkaline fuel cells,[40,41] the hydrogen conversion at the anode can also be realized with low kinetic overpotentials.[42] Thus, in the three different types of fuel cells (PEM, alkaline, and solid oxide) smaller kinetic overvoltages of the electrochemical hydrogen oxidation than the ohmic drops in the anodes can occur, which can lead to parasitic electrochemical currents in the anode.

SUMMARY

In this study, the resistivities of the proton conduction through samples with the same compositions as PEM fuel cell catalyst layers were measured in a hydrogen atmosphere. The resistivities of the samples were up to ten times smaller than those of Nafion membranes. This effect was explained by parasitic electrochemical currents, which originated from the electrochemical hydrogen oxidation and evolution within the samples. The driving force for these reactions was ascribed to a potential difference between the electric phase and the ionic phase of the samples, which is caused by a smaller resistance for the electron conduction than that of the proton conduction. The occurrence of such parasitic electrochemical currents in the anode of fuel cells was postulated, when the difference of the ohmic drops of the ion and electron conduction is higher than the kinetic overvoltage of the hydrogen oxidation reaction. These parasitic electrochemical currents increase the ohmic drop in the anode and kinetic losses of the electrochemical hydrogen oxidation. A reduction of the thickness of the anode decreases its total ion resistance and thus might decrease or even avoid the parasitic electrochemical currents. In fuel cells with alkaline or solid oxide electrolyte the occurrence of parasitic electrochemical currents within the anode was also postulated and discussed.

ASSOCIATED CONTENT

Supporting Information

The sample preparation, the experimental setup, and the characterization of the experimental methods will be discussed in detail. The Supporting Information is available free of charge on the ACS Publications website at DOI: 10.1021/acsami.5b02182.

AUTHOR INFORMATION

Corresponding Author

*Phone: +49 2461 619802. Fax: +49 2461 618161. E-mail: m.schalenbach@fz-juelich.de.

Notes

The authors declare no competing financial interest.

ACKNOWLEDGMENTS

This research has been supported by the German Federal Ministry of Economics and Technology under Grant No. 03ESP106A.

REFERENCES

(1) Kulikovsky, A. A. The Regimes of Catalyst Layer Operation in a Fuel Cell. *Electrochim. Acta* **2010**, *55*, 6391−6401.
(2) El Hannach, M.; Prat, M.; Pauchet, J. Pore Network Model of the Cathode Catalyst Layer of Proton Exchange Membrane Fuel Cells: Analysis of Water Management and Electrical Performance. *Int. J. Hydrogen Energy* **2012**, *37*, 18996−19006.
(3) Marr, C.; Li, X. Composition and Performance Modelling of Catalyst Layer in a Proton Exchange Membrane Fuel Cell. *J. Power Sources* **1999**, *77*, 17−27.
(4) Um, S.; Wang, C. Three-Dimensional Analysis of Transport and Electrochemical Reactions in Polymer Electrolyte Fuel Cells. *J. Power Sources* **2004**, *125*, 40−51.
(5) Yi, J. S.; Nguyen, T. V. Multicomponent Transport in Porous Electrodes of Proton Exchange Membrane Fuel Cells Using the Interdigitated Gas Distributors. *J. Electrochem. Soc.* **1999**, *146*, 38−45.
(6) Fischer, A.; Jindra, J.; Wendt, H. Porosity and Catalyst Utilization of thin Layer Cathodes in Air operated PEM-fuel cells. *J. Appl. Electrochem.* **1998**, *28*, 277−282.
(7) Greeley, J.; Jaramillo, T. F.; Bonde, J.; Chorkendorff, I. B.; Nørskov, J. K. Computational High-Throughput Screening of

DOI: 10.1021/acsami.5b02182
ACS Appl. Mater. Interfaces 2015, 7, 15746−15751

Electrocatalytic Materials for Hydrogen Evolution. *Nat. Mater.* **2006**, *5*, 909−13.
(8) Nørskov, J. K.; Rossmeisl, J.; Logadottir, A.; Lindqvist, L.; Kitchin, J.; Bligaard, T.; Jonsson, H. Origin of the Overpotential for Oxygen Reduction at a Fuel-Cell Cathode. *J. Phys. Chem. B* **2004**, *108*, 17886−17892.
(9) Nesselberger, M.; Ashton, S.; Meier, J. C.; Katsounaros, I.; Mayrhofer, K. J. J.; Arenz, M. The Particle Size Effect on the Oxygen Reduction Reaction Activity of Pt Catalysts: Influence of Electrolyte and Relation to Single Crystal Models. *J. Am. Chem. Soc.* **2011**, *133*, 17428−17433.
(10) Vidal-iglesias, F. J.; Aran-Ais, R. M.; Solla-Gullon, J.; Herrero, E.; Feliu, J. M. Electrochemical Characterization of Shape-Controlled Pt Nanoparticles in Different Supporting Electrolytes. *ACS Catal.* **2012**, *2*, 901−910.
(11) Antolini, E. Carbon Supports for Low-Temperature Fuel Cell Catalysts. *Appl. Catal., B* **2009**, *88*, 1−24.
(12) Litster, S.; McLean, G. PEM Fuel Cell Electrodes. *J. Power Sources* **2004**, *130*, 61−76.
(13) Rajalakshmi, N.; Dhathathreyan, K. Catalyst Layer in PEMFC Electrodes - Fabrication, Characterisation and Analysis. *Chem. Eng. J.* **2007**, *129*, 31−40.
(14) Mauritz, K. A.; Moore, R. B. State of Understanding of Nafion®. *Chem. Rev.* **2004**, *104*, 4535−85.
(15) Mehta, V.; Cooper, J. S. Review and Analysis of PEM Fuel Cell Design and Manufacturing. *J. Power Sources* **2003**, *114*, 32−53.
(16) Smitha, B.; Sridhar, S.; Khan, A. Solid Polymer Electrolyte Membranes for Fuel Cell Applications - A Review. *J. Membr. Sci.* **2005**, *259*, 10−26.
(17) O'Hayre, R.; Barnett, D. M.; Prinz, F. B. The Triple Phase Boundary. *J. Electrochem. Soc.* **2005**, *152*, A439.
(18) Morris, D. R. P.; Liu, S. P.; Gonzalez, D. V.; Gostick, J. T. Effect of Water Sorption on the Electronic Conductivity of Porous Polymer Electrolyte Membrane Fuel Cell Catalyst Layers. *ACS Appl. Mater. Interfaces* **2014**, *6*, 18609−18618.
(19) Eikerling, M.; Kornyshev, A. A.; Stimming, U. Electrophysical Properties of Polymer Electrolyte Membranes: A Random Network Model. *J. Phys. Chem. B* **1997**, *101*, 10807−10820.
(20) Jorn, R.; Voth, G. A. Mesoscale Simulation of Proton Transport in Proton Exchange Membranes. *J. Phys. Chem. C* **2012**, *116*, 10476−10489.
(21) Kreuer, K.-D. The Role of Internal Pressure for the Hydration and Transport Properties of Ionomers and Polyelectrolytes. *Solid State Ionics* **2013**, *252*, 93−101.
(22) Eikerling, M. H.; Berg, P. Poroelectroelastic Theory of Water Sorption and Swelling in Polymer Electrolyte Membranes. *Soft Matter* **2011**, *7*, 5976.
(23) Divisek, J.; Eikerling, M.; Schmitz, V. M. H.; Stimming, U.; Volfkovichb, Y. M. A Study of Capillary Porous Structure and Sorption Properties of Nafion® Proton-Exchange Membranes Swollen in Water. *J. Electrochem. Soc.* **1998**, *145*, 2677−2683.
(24) Silva, R.; De Francesco, M.; Pozio, A. Tangential and Normal Conductivities of Nafion® Membranes used in Polymer Electrolyte Fuel Cells. *J. Power Sources* **2004**, *134*, 18−26.
(25) Sone, Y.; Ekdinge, P.; Simonsson, D. Proton Conductivily of Nafion® 117 as Measured by a Four-Electrode AC Impedance Method. *J. Electrochem. Soc.* **1996**, *143*, 1254−1259.
(26) Anantaraman, A.; Gardner, C. Studies on Ion-Exchange Membranes. Part 1. Effect of Humidity on the Conductivity of Nafion®. *J. Electroanal. Chem.* **1996**, *414*, 115−120.
(27) Boyer, C.; Gamburzev, S.; Velev, O.; Srinivasan, S.; Appleby, A. J. Measurements of Proton Conductivity in the Active Layer of PEM Fuel Cell Gas Diffusion Electrodes. *Electrochim. Acta* **1998**, *43*, 3703−3709.
(28) Neyerlin, K. C.; Gu, W.; Jorne, J.; Gasteiger, H. A. Study of the Exchange Current Density for the Hydrogen Oxidation and Evolution Reactions. *J. Electrochem. Soc.* **2007**, *154*, B631.
(29) Zhang, J.; Tang, Y.; Song, C.; Zhang, J.; Wang, H. PEM Fuel Cell Open Circuit Voltage (OCV) in the Temperature Range of 23°C to 120°C. *J. Power Sources* **2006**, *163*, 532−537.
(30) Mann, R. F.; Amphlett, J. C.; Hooper, M. A.; Jensen, H. M.; Peppley, B. A.; Roberge, P. R. Development and Application of a Generalised Steady-State Electrochemical Model for a PEM Fuel Cell. *J. Power Sources* **2000**, *86*, 173−180.
(31) Springer, T. E.; Zawodzinski, T. A.; Gottesfeld, S. Polymer Electrolyte Fuel Cell Model. *J. Electrochem. Soc.* **1991**, *138*, 2334−42.
(32) Goodenough, J. B.; Huang, Y.-H. Alternative Anode Materials for Solid Oxide Fuel Cells. *J. Power Sources* **2007**, *173*, 1−10.
(33) Zhu, W.; Deevi, S. A Review on the Status of Anode Materials for Solid Oxide Fuel Cells. *Mater. Sci. Eng., A* **2003**, *362*, 228−239.
(34) Wilson, J. R.; Kobsiriphat, W.; Mendoza, R.; Chen, H.-Y.; Hiller, J. M.; Miller, D. J.; Thornton, K.; Voorhees, P. W.; Adler, S. B.; Barnett, S. A. Three-Dimensional Reconstruction of a Solid-Oxide Fuel-Cell Anode. *Nat. Mater.* **2006**, *5*, 541−4.
(35) Weber, A.; Ivers-Tiffée, E. Materials and Concepts for Solid Oxide Fuel Cells (SOFCs) in Stationary and Mobile Applications. *J. Power Sources* **2004**, *127*, 273−283.
(36) Kim, J.-W.; Virkar, A. V.; Fung, K.-Z.; Mehta, K.; Singhal, S. C. Polarization Effects in Intermediate Temperature, Anode-Supported Solid Oxide Fuel Cells. *J. Electrochem. Soc.* **1999**, *146*, 69−78.
(37) Huang, Y.-H.; Dass, R. I.; Xing, Z.-L.; Goodenough, J. B. Double Perovskites as Anode Materials for Solid-Oxide Fuel Cells. *Science* **2006**, *312*, 254−257.
(38) Sun, C.; Stimming, U. Recent Anode Advances in Solid Oxide Fuel Cells. *J. Power Sources* **2007**, *171*, 247−260.
(39) Zhao, F.; Virkar, a. Dependence of Polarization in Anode-Supported Solid Oxide Fuel Cells on Various Cell Parameters. *J. Power Sources* **2005**, *141*, 79−95.
(40) Mclean, G. F.; Niet, T.; Djilali, N. An Assessment of Alkaline Fuel Cell Technology. *Int. J. Hydrogen Energy* **2002**, *27*, 507−526.
(41) Bidault, F.; Brett, D.; Middleton, P.; Brandon, N. Review of Gas Diffusion Cathodes for Alkaline Fuel Cells. *J. Power Sources* **2009**, *187*, 39−48.
(42) Jo, J.-H.; Yi, S.-C. A Computational Simulation of an Alkaline Fuel Cell. *J. Power Sources* **1999**, *84*, 87−106.

DOI: 10.1021/acsami.5b02182
ACS Appl. Mater. Interfaces 2015, 7, 15746−15751